Published as Adv. Synth. Catal. 2016, 358, 3231-3243. doi.org/10.1002/adsc.201600621

Coupling of CO_2 with Epoxides Efficiently Catalyzed by Thioether-Triphenolate Bimetallic Iron(III) Complexes: Catalyst Structure - Reactivity Relationship and Mechanistic DFT Study

Francesco Della Monica[†], Sai V.C. Vummaleti[‡], Antonio Buonerba[†§], Assunta De Nisi[§¶], Magda Monari[§¶], Stefano Milione[†§], Alfonso Grassi[†§], Luigi Cavallo[‡], Carmine Capacchione[†§]**

[†] Dipartimento di Chimica e Biologia "Adolfo Zambelli", Università degli Studi di Salerno, via Giovanni Paolo II, 84084 Fisciano(SA), Italy

[‡] KAUST Catalysis Center, King Abdullah University of Science and Technology, Thuwal 23955-6900, Saudi Arabia

[§] Interuniversity Consortium Chemical Reactivity and Catalysis, CIRCC, via Celso Ulpiani 27, 70126 (BA), Italy.

[¶] Dipartimento di Chimica G. Ciamician, Alma Mater Studiorum, Università di Bologna, via Selmi 2, Bologna, Italy

Published as Adv. Synth. Catal. 2016, 358, 3231-3243. doi.org/10.1002/adsc.201600621

KEYWORDS: carbon dioxide; epoxides; cycloaddition; coupling; mechanism; cyclic carbonates; DFT.

ABSTRACT: A series of dinuclear Fe(III) complexes supported by thioether-triphenolate ligands have been prepared to attain highly Lewis acidic catalysts. In combination with tetrabutylammonium bromide (TBAB) they are highly active catalysts in the synthesis of cyclic organic carbonates through the coupling of carbon dioxide to epoxides with the highest initial turnover frequencies reported to date for the conversion of propylene oxide to propylene carbonate for iron based catalysts (5200 h^{-1}; 120 °C, 2MPa, 1h). In particular these complexes show to be highly selective catalyst for the coupling of carbon dioxide to internal oxiranes affording the corresponding cyclic carbonates in good yield and with retention of the initial stereochemical configuration. Density functional theory (DFT) investigation provides a rational for the relative high activity found for these Fe(III) complexes, showing the fundamental role of the hemilabile sulfur atom in the ligand skeleton to promote reactivity. Notably, in spite of the dinuclear nature of the catalyst precursor only one metal center is involved in the catalytic cycle.

Published as Adv. Synth. Catal. 2016, 358, 3231-3243. doi.org/10.1002/adsc.201600621

INTRODUCTION

Above the last two decades an increasing interest in the use of carbon dioxide as chemical feedstock has engendered intensive efforts, in both academia and industry, for the search of new synthetic pathways to useful compounds and polymers.[1] The main problem slowing the development of a chemistry based on CO_2 as C1 building block lies in the kinetic and thermodynamic stability of this molecule that renders its conversion into valuable chemicals energetically unfavorable. Similarly to other industrially relevant processes, the clue to overcome the kinetic inertness of the carbon dioxide is the implementation of efficient catalytic systems that allow the conversion of CO_2 to useful products under blander reaction conditions. In this context, one of the most promising synthetic routes is the development of efficient catalytic systems able to promote the coupling of CO_2 with oxiranes giving the corresponding cyclic organic carbonates (COCs)[2] or polycarbonates.[3] In particular COCs have many applications, such as polar aprotic green solvents, electrolytes in lithium–ion batteries, and as chemical intermediates in the synthesis of other small molecules or polymers. As a matter of fact, a large repertoire of catalytic systems mainly based on transition metal complexes combined with a nucleophile (quaternary ammonium salts and phosphonium salts) as co-catalyst has been developed and shown to be highly active and selective for the cycloaddition of CO_2 to epoxides.[2] It is worth noting that the most studied and active complexes are based on metals such as chromium, cobalt, zinc, magnesium or niobium.[2d] These are metals that have risen health and environment concerns, and have also been recently defined as endangered elements *i.e.* metals that will be not available anymore at affordable price in the next future.[4] This situation has triggered the search of new, greener and inexpensive catalytic systems able to efficiently promote this reaction. The two most promising approaches to achieve this goal are: 1) the

Published as Adv. Synth. Catal. 2016, 358, 3231-3243. doi.org/10.1002/adsc.201600621

development of metal-free organocatalytic systems,[5] 2) the use of complexes based on Earth-crust abundant metals (Fe, Al, Ti, Ca).[2e] In spite of the growing number of organocatalysts, the presence of a Lewis acidic metal center that activates the opening of the oxirane ring offers still advantages in terms of high activity, low catalyst loading and even milder reaction conditions. In this field aluminum based catalysts have been extensively investigated.[6] In particular, the bimetallic aluminum(salen) complex developed by North[7] and coworkers and the aluminum amino-tris(phenolate) complex reported by Kleji[8] and coworkers have been shown to be highly active and versatile catalysts for the formation of cyclic carbonates. Conversely, notwithstanding the growing interest in the use of iron in catalysis,[9] the examples of iron based catalysts for the formation of cyclic carbonates from CO_2 and epoxides are rather scarce.[10]

We have recently reported on new catalysts based on dinuclear Fe(III) complexes (complexes **1-3**; Scheme 1), bearing dithioether-triphenolate-based ligands in combination with tetrabutylammonium bromide (TBAB), which have shown to be high active and versatile in the synthesis of COCs.[11]

Scheme 1. Synthesis of the proligands **L1-L6** and the correspondent Iron(III) complexes **1-6**.

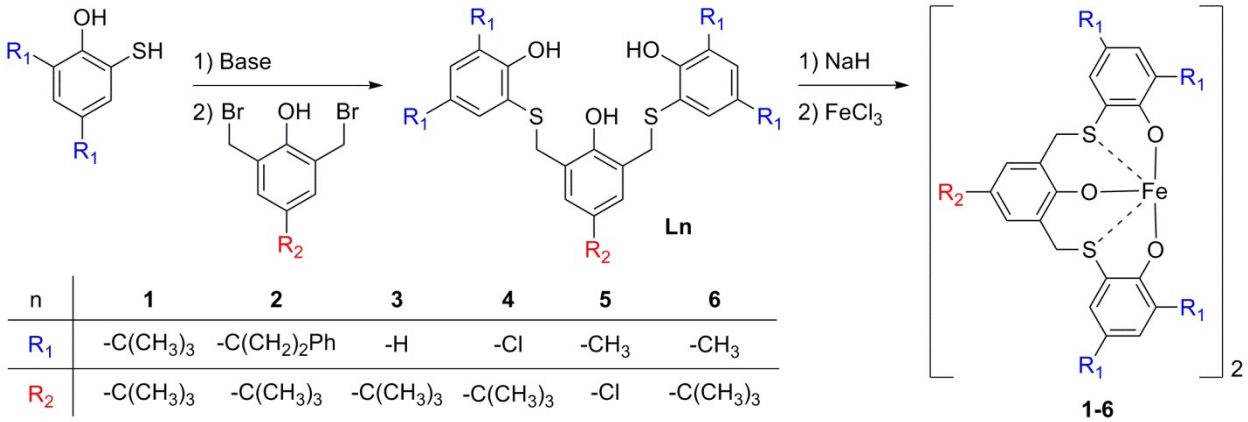

n	1	2	3	4	5	6
R_1	$-C(CH_3)_3$	$-C(CH_2)_2Ph$	-H	-Cl	$-CH_3$	$-CH_3$
R_2	$-C(CH_3)_3$	$-C(CH_3)_3$	$-C(CH_3)_3$	$-C(CH_3)_3$	-Cl	$-C(CH_3)_3$

Published as Adv. Synth. Catal. 2016, 358, 3231-3243. doi.org/10.1002/adsc.201600621

These results have shown that it is possible to obtain efficient catalysts for the cycloaddition of CO_2 to epoxides based on iron complexes, and that the presence of the hemilabile Fe-S bond in the catalyst precursor has a beneficial role in the subsequent epoxide coordination to the metal center, promoting the formation of the cyclic carbonate in the presence of the nucleophilic co-catalyst. Here we report the synthesis and complete characterization of three novel iron(III) complexes **4**-**6** bearing dithioether-triphenolate ligands and their use as catalysts for the coupling of CO_2 with epoxides and compare their performances with known complexes **1**-**3** iron(III) complexes under the same reaction conditions. In combination with TBAB and under optimized reaction conditions, they show high activity in the coupling of various terminal epoxides with CO_2. In addition, they also convert various internal epoxides affording the corresponding carbonates in good yields and with high stereoselectivity. Density functional theory calculations (DFT) reveal that in spite of the bimetallic nature of the catalyst precursor only one metal center is involved in the catalytic cycle.

EXPERIMENTAL SECTION

All manipulation involving air- and/or moisture-sensitive compounds were performed under nitrogen atmosphere using standard Schlenk technique and a MBraun glovebox. Toluene (99.5%; Sigma-Aldrich) and THF (99%; Sigma-Aldrich) were used as received or refluxed for 48 h over sodium or sodium ketyls and distilled before use for moisture- and oxygen-sensitive reactions. All other reagents were used as received (TCI or Sigma-Aldrich) or distilled under reduced pressure over calcium hydride. The ligand precursors: 2,6-[[3,5-di-tert-butyl-2-hydroxyphenyl]thio]-4-tert-butylphenol (**L1**), 2,6-[[3,5-*bis*-α,α'-dimethylbenzyl-2-

Published as Adv. Synth. Catal. 2016, 358, 3231-3243. doi.org/10.1002/adsc.201600621

hydroxyphenyl]thio]-4-tert-butylphenol (**L2**), 2,6-[[2-hydroxyphenyl]thio]-4-tert-butylphenol (**L3**) and the corresponding iron(III) complexes (**1**, **2**, **3**, Scheme 2) were synthesized according to the reported procedures.[11] Deuterated solvents were purchased from Euriso-Top or Sigma-Aldrich and used as received. NMR spectra were collected on Bruker Avance spectrometers (600, 400, 300 or 250 MHz for ^{1}H): the chemical shifts were referenced to tetramethylsilane (TMS) as external reference using the residual protio signal of the deuterated solvents. Measurements of effective magnetic moments were performed on a Bruker Avance 600 MHz spectrometer at 25 °C in toluene-d_8 using a 5 mm Wilmad coaxial insert NMR tube.[12] Solutions of the complex **4** (2.22 mM), **5** (2.29 mM) and **6** (2.16 mM) in toluene-d_8 with 1 % (v/v) of TMS were prepared under nitrogen atmosphere. The effective magnetic moment (μ_{eff}) was calculated from $\mu_{eff} = 8\chi_g M_w T$, where χ_g (cm^3 g^{-1}) is the corrected molar susceptibility derived from $\chi_g = 3\Delta_f/4\pi f_o C M_w + \chi_o$. Δ_f is the shift in frequency (Hz) of the residual protio signal of the solvent in presence of the complex from the value of the pure solvent, C and M_w are respectively the concentration (mol cm^{-3}) and the molecular weight of the complex (g mol^{-1}), f_o is the operating frequency of the spectrometer (Hz), and χ_o is the mass susceptibility of the pure solvent (−0.6179 × 10^{-6} cm^3 g^{-1} for toluene-d_8). $4\pi/3$ is the shape factor for a cylindrical sample in a superconducting magnet. The magnetic susceptibilities of all the complexes **1**-**6** in the solid state were measured using a Sherwood Scientific MK 1 magnetic susceptibility balance by means of the Faraday method based on the following equation: $f_s / f_r = (\chi_s \cdot m_s) / (\chi_r \cdot m_r)$ where f_s, χ_s and m_s are the magnetic force, the specific susceptibility and the mass of the sample, while f_r, χ_r and m_r are the magnetic force, the specific susceptibility and the mass of $CuSO_4 \cdot 5H_2O$ used as reference compound with a value of $\chi_r = 6.00 \cdot 10^{-6}$ cm^3 · g^{-1}.[13] Magnetic moments were calculated using the following equation: $\mu_{eff} = 2.828 \cdot (T \cdot \chi_m)^{1/2}$, where μ_{eff} is the effective

Published as Adv. Synth. Catal. 2016, 358, 3231-3243. doi.org/10.1002/adsc.201600621

magnetic moment, T is the absolute temperature and χ_m is the molar susceptibility. Effective magnetic moments values for all complexes in both solution and solid state are listed in Table S2 of the supporting information. Elemental analysis was performed on a CHNS Thermo Scientific Flash EA 1112 equipped with a thermal conductivity detector. ESI-MS spectra were acquired on a Quattro *micro*™ API triple quadrupole mass spectrometer from Waters equipped with electrospray ion source, using anhydrous acetonitrile as solvent. FT-IR measurements were carried out on a Bruker Vertex 70 spectrometer equipped with DTGS detector and a Ge/KBr beam splitter. The samples were analyzed in chloroform solutions or in the solid state as KBr disks. UV-Vis spectra were collected on a PerkinElmer Lambda EZ 201 spectrophotometer.

Synthesis of the pro-ligand 2,6-[[3,5-dichloro-2-hydroxyphenyl]thio]-4-*tert*-butylphenol (L4, Scheme 2). The pro-ligand **L4** was synthesized using a modification of the previously reported procedure for **L1**.[11] A 100 mL two-neck round-bottom flask equipped with condenser and magnetic stirring bar was charged with 0.76 g of 2-mercapto-4,6-dichlorophenol (3.9 mmol) dissolved in 4 mL of ethanol, 1.4 g of Cs_2CO_3 (4.3 mmol) and the mixture was refluxed for 2 hours until complete dissolution of Cs_2CO_3. 0.66 g of 2,6-dibromomethyl-4-*tetr*-butylphenol (1.96 mmol) dissolved in 2 mL of ethanol were slowly added at 0 °C and the mixture was refluxed overnight. The solvent was distilled off, water was added until dissolution of the residue and the aqueous phase extracted twice with CH_2Cl_2. The combined organic phases were dried with $MgSO_4$ and, after evaporation of the solvent, the product was purified by column chromatography (eluent: CH_2Cl_2) and recovered as a white solid. Yield: 0.94 g, 85 %. ^{1}H-NMR (600 MHz, CD_2Cl_2, 25 °C): δ 1.12 (9H, s); 4.04 (4H, s); 6.80 (2H, s, Ar-H); 7.19 (2H, d, Ar-H); 7.32 (2H, d, Ar-H). ^{13}C-NMR (600 MHz, CD_2Cl_2, 25 °C): δ 31.36; 34.21; 36.55; 121.08; 121.98;

Published as Adv. Synth. Catal. 2016, 358, 3231-3243. doi.org/10.1002/adsc.201600621

123.05; 124.99; 127.99; 130.83; 134.07; 143.75; 150.61; 152.14. EA for $C_{24}H_{22}Cl_4O_3S_2$ calc.: C, 51.08; H, 3.93; S 11.36; found: C, 51,02, H, 3.82; S, 11.25. Mass spectrum: 586.7 m/z (MNa^+).

Synthesis of the pro-ligand 2,6-[[3,5-dimethyl-2-hydroxyphenyl]thio]-4-chlorophenol (L5, Scheme 2). The pro-ligand **L5** was synthesized using a modification of the previously reported procedure for **L1**.[11] A 100 mL two-neck round-bottom flask equipped with condenser and magnetic stirring bar was charged with 0.80 g of 2-mercapto-4,6-dimethylphenol (5.2 mmol) dissolved in 13 mL of DMF, 0.90 g of K_2CO_3 (6.5 mmol) and the resulting mixture was refluxed for 2 hours. 0.82 g of 2,6-dibromomethyl-4-chlorolphenol (2.6 mmol) dissolved in 7 mL of DMF were slowly added at 0 °C and was refluxed overnight. The solvent was distilled off, water was added and the aqueous phase extracted twice with CH_2Cl_2. The combined organic phases were dried with $MgSO_4$ and, the product was recovered after evaporation of the solvent as a white solid. Yield: 0.97 g, 81 %. ^{1}H-NMR (400 MHz, CD_2Cl_2, 25 °C): 2.17 (6H, s); 2.23 (6H,s); 3.86 (4H, s); 6.11 (1H, s broad, -OH); 6.54 (2H, s broad, -OH); 6.76 (2H, s, Ar-H); 6.92 (2H, s, Ar-H); 6.95 (2H,s, Ar-H). ^{13}C-NMR (400 MHz, CD_2Cl_2, 25 °C): δ 16.48; 20.36; 36.52; 116.53; 124.38; 125.27; 126.23; 129.69; 129.89; 133.83; 134.03; 151.25; 153.23. EA for $C_{24}H_{25}Cl_2O_3S_2$ calc.: C, 62.52; H, 5.47; S 13.91; found: C, 62.49; H, 5.42; S, 13.87. Mass spectrum: 483.6 m/z (MNa^+).

Synthesis of the pro-ligand 2,6-[[3,5-dimethyl-2-hydroxyphenyl]thio]-4-*tert*-butylphenol (L6, Scheme 2). The pro-ligand **L6** was synthesized using the previously reported procedure for **L1**.[11] A 100 mL two-neck round-bottom flask equipped with condenser and magnetic stirring bar was charged with 3.14 g of 2-mercapto-4,6-dimethylphenol (20.4 mmol) dissolved in 20 mL of ethanol, 0.90 g of NaOH (22.4 mmol) and the mixture was refluxed about 1 hour until complete dissolution of the hydroxide. 3.42 g of 2,6-dibromomethyl-4-*tetr*-butylphenol (10.2 mmol)

Published as Adv. Synth. Catal. 2016, 358, 3231-3243. doi.org/10.1002/adsc.201600621

dissolved in 15 mL of ethanol were slowly added at 0 °C and the mixture heated to the reflux of the solvent that was kept overnight. The solvent was distilled off, water was added until dissolution of NaBr by-product and the aqueous phase extracted twice with CH_2Cl_2. The combined organic phases were dried with $MgSO_4$, after evaporation of the solvent the product was purified by column chromatography (petroleum ether : ethyl acetate = 95:5) and recovered as a white solid. Yield: 2.82 g, 57.3 %. ^{1}H-NMR (400 MHz, CD_2Cl_2, 25 °C): δ 1.05 (9H, s); 2.14 (6H, s); 2.17 (6H,s); 3.91 (4H, s); 5.79 (1H, s, -OH); 6.60 (2H, s, -OH); 6.69 (2H, s, Ar-H); 6.91 (4H,s, Ar-H). ^{13}C-NMR (400 MHz, CD_2Cl_2, 25 °C): δ 16.47; 20.34; 31.27; 34.08; 37.17; 117.18; 124.04; 124.20; 127.55; 129.60; 133.75; 134.12; 143.46; 150.09; 153.56. EA for $C_{28}H_{34}O_3S_2$ calc.: C, 69.67; H, 7.10; S 13.29; found: C, 69.55; H, 7.09; S, 13.18. Mass spectrum: 505.0 m/z (MNa^+).

Synthesis of the iron(III) complex 4 (Scheme 2). The complex **4** was synthesized using the same procedure previously reported for complex **1**.[11] Pro-ligand **L4** (0.54 g; 0.96 mmol) was dissolved in THF (30mL). The solution was added to a suspension of sodium hydride (0.082 g; 3.4 mmol) in THF (20 mL) and the mixture stirred at room temperature overnight. The resulting suspension was filtered through celite and slowly added at room temperature to 0.148 g of anhydrous iron(III) chloride (0.91 mmol) dissolved in 15 mL of THF. The rapid change of the color to blue was observed and the reaction kept overnight at room temperature. The mixture was then filtered through a celite path and the solvent removed under reduced pressure affording a deep purple crystalline solid. Yield: 0.44 g, 78 %. EA for $C_{48}H_{38}Fe_2Cl_8O_6S_4$ calc.: C, 46.70; H, 3.10; S, 10.39; found: C, 46.61; H, 3.03; S, 10.35. Mass spectrum: 981.2 m/z (MNa+); 1354.8 m/z($M(CH_3CN)_2K^+$). UV-Vis: ε_{585} = 5441 L mol^{-1} cm^{-1}.

Published as Adv. Synth. Catal. 2016, 358, 3231-3243. doi.org/10.1002/adsc.201600621

Synthesis of the iron(III) complex 5 (Scheme 2). The complex **5** was synthesized using the same procedure previously reported for complex **1**.[11] Pro-ligand **L5** (0.94 g; 2.04 mmol) was dissolved in THF (70mL). The solution was added to a suspension of sodium hydride (0.17 g; 7.08 mmol) in THF (30 mL) and the mixture stirred at room temperature overnight. The resulting suspension was filtered through celite and slowly added at room temperature to 0.325 g of anhydrous iron(III) chloride (2.0 mmol) dissolved in 30 mL of THF. The rapid change of the color to the blue was observed and the reaction kept overnight. The mixture was then filtered through celite and the solvent removed under reduced pressure affording a deep purple crystalline solid. Yield: 0.83 g, 80 %. EA for $C_{48}H_{44}Fe_2Cl_2O_6S_4$ calc.: C, 56.10; H, 4.32; S, 12.48; found: C, 56.02; H, 4.28; S, 12.39. Mass spectrum: 981.2 m/z (MNa+). UV-Vis: ε_{596} = 4757 L mol^{-1} cm^{-1}.

Synthesis of the iron(III) complex 6 (Scheme 2). The complex **6** was synthesized using the same procedure previously reported for complex **1**.[11] Pro-ligand **L6** (1.62 g; 3.56 mmol) was dissolved in THF (100mL). The solution was added to a suspension of sodium hydride (0.30 g; 12.5 mmol) in THF (70 mL) and the mixture stirred at room temperature overnight. The resulting suspension was filtered through celite and slowly added at room temperature to 0.567 g of anhydrous iron(III) chloride (3.50 mmol) dissolved in 100 mL of THF. The rapid change of the color to the deep purple was observed and the reaction kept overnight. The mixture was then filtered through celite and the solvent removed under reduced pressure affording a deep purple crystalline solid. Yield: 1.60 g, 85 %. EA for $C_{56}H_{62}Fe_2O_6S_4$ calc.: C, 62.30; H, 5.83; S, 11.98; found: C, 62.20; H, 5.78; S, 11.89. Mass spectrum: 1072.1 m/z (MH+). UV-Vis: ε_{586} = 4962 L mol^{-1} cm^{-1}.

Published as Adv. Synth. Catal. 2016, 358, 3231-3243. doi.org/10.1002/adsc.201600621

Typical procedure for CO_2/epoxide coupling to cyclic carbonates catalyzed by 6/TBAB (referred to entry 15, Table S1). A 60 mL stainless steel pressure reactor equipped with a magnetic stirring bar was charged, under CO_2 atmosphere, with 7.7 mg of catalyst **6** (7.15×10^{-6} mol) and 23.0 mg of TBAB (7.15×10^{-5} mol) dissolved in 5.0 mL of PO (7.15×10^{-2} mol). The reaction mixture was pressurized with CO_2 at 2.0 MPa and stirred at 120 °C for 1 h. The reactor was cooled with ice, the CO_2 released, 1.0 mL of mesitylene (7.15×10^{-3} mol) was added as an internal standard and the mixture was analyzed by ^{1}H NMR spectroscopy using $CDCl_3$ as solvent. Yield 52.0 %.

Crystallographic Data Collection and Structure Determination for complex 6. The X-ray intensity data were measured on a Bruker SMART Apex II CCD area detector diffractometer. Cell dimensions and the orientation matrix were initially determined from a least-squares refinement on reflections measured in three sets of 20 exposures, collected in three different ω regions, and eventually refined against all data. A full sphere of reciprocal space was scanned by 0.3° ω steps. The software SMART[14] was used for collecting frames of data, indexing reflections, and determination of lattice parameters. The collected frames were then processed for integration by the SAINT program[14] and an empirical absorption correction was applied using SADABS.[15] The structure was solved by direct methods (SIR 2004)[16] and subsequent Fourier syntheses and refined by full-matrix least-squares on F^2 (SHELXTL)[17], using anisotropic thermal parameters for all non-hydrogen atoms. All hydrogen atoms were added in calculated positions, included in the final stage of refinement with isotropic thermal parameters, U(H) = 1.2 U_{eq}(C) [U(H) = 1.5 U_{eq}(C-Me)], and allowed to ride on their carrier carbons. Crystal data and details of the data collection for complex **6** are reported in Table S3 and Table S4.

Published as Adv. Synth. Catal. 2016, 358, 3231-3243. doi.org/10.1002/adsc.201600621

Computational Protocol. All the DFT geometry optimizations were performed at the GGA level with the Gaussian09 set of programs,[18] using the BP86 functional of Becke and Perdew.[19] The electronic configuration of the molecular systems was described with the split-valence plus one polarization function basis set of Ahlrichs for H, C, N, O, S and Br (SVP keyword in Gaussian).[20] For Fe, we used the small-core, quasi-relativistic Stuttgart–Dresden effective core potential, with the associated triple-ζ valence basis set (SDD keywords in Gaussian09).[21] Geometry optimizations were performed without symmetry constraints, and the characterization of the located stationary points was performed by analytical frequency calculations. For better energetics, energies were re-evaluated via single point calculations on the BP86/SVP optimized geometries with the triple-ζ plus one polarization function basis set proposed by Ahlrichs (TZVP keyword in Gaussian)[22] using the M06 functional.[23] Solvent effects (propylene oxide) were estimated with the polarizable continuum solvation model PCM.[24] To this M06/TZVP electronic energy in solvent, zero point energy and thermal corrections were included from the gas-phase frequency calculations at the BP86/SVP level.[25] All the calculations were performed with an unrestricted DFT formalism, assuming the two Fe centers in a high spin state.

RESULTS AND DISCUSSION

Synthesis and Characterization of the iron(III) complexes 4-6

The Lewis acidity of the metal center, according to the widely accepted reaction mechanism,[2d] should play a crucial role in the determination of the catalytic activity for the cycloaddition of carbon dioxide to oxiranes. Indeed, with the aim to increase the Lewis acidity of the iron atoms, we decided to modify the pro-ligand structure introducing an electron withdrawing substituent, such as chlorine, on the lateral (**L4**) and central (**L5**) phenol rings, in order to evaluate the impact

Published as Adv. Synth. Catal. 2016, 358, 3231-3243. doi.org/10.1002/adsc.201600621

on the catalytic activity in the formation of the cyclic carbonates. The methyl-substituted pro-ligand (**L6**) was also synthesized to have an alkyl-substituted complex (**6**) with a steric hindrance comparable with that of the chlorine substituted one (**4**). The pro-ligands **L4-6**, were synthesized by modification of the procedure previously reported (Scheme 2).[11] All the new pro-ligands were fully characterized by nuclear magnetic resonance (^{1}H, ^{13}C and ^{1}H-^{13}C HSQC NMR), mass spectrometry (ESI-MS), elemental analysis (EA) and infrared spectroscopy (FT-IR) (see Supporting Information). Complexes **4-6**, were obtained by reaction of an equimolar amount of $FeCl_3$ with the sodium salt of the corresponding pro-ligand in THF, obtained from the reaction of the ligand precursor with 3 equivalents of sodium hydride. All the products were recovered in good yields (from 78 to 85%), as deep-blue powder. Complexes **4-6** were characterized by elemental analysis. Furthermore, by comparison of the FT-IR spectra of complexes **4-6** with those of the corresponding ligands , disappearance of the hydroxyl group vibration around 3300 cm^{-1} confirms the formation of the desired complexes. Moreover the shift of the vibration bands diagnostic of the alkyl-sulphide moiety (see Supporting Information), indicates the coordination of the sulfur atoms to the iron centers. Indeed the UV-Vis spectra of the complexes only show a strong ligand-to-metal charge transfer absorption and no *d-d* transition as expected for two hexacoordinated HS iron(III) centers. The ESI-MS analysis was consistent with the formation of dinuclear species (Figures S14-S16-S18). In addition the values of the effective magnetic moments determined using the Evans method[12] in toluene-d_8 at 30 °C, are comparable with the calculated value for two isolated high spin (HS) iron(III) centers (8.37 μB).[26] Notably, the magnetic moments measured in the solid state with a Johnson-Matthey balance by using the Faraday's method[13] are in good agreement with values obtained in solution confirming that the complexes possess a dimeric structure both in the solid state and in solution (see Table S2).

Published as Adv. Synth. Catal. 2016, 358, 3231-3243. doi.org/10.1002/adsc.201600621

Finally addition of a large excess of a strong coordinating species mimicking the epoxide substrate, such as pyridine, to a toluene solution of **6** (50 equivalents with respect to **6**) does not produce any change of the UV-Vis spectrum profile underlying the stability of the dimeric structure in solution (see Figure S21-23). Single crystals of **6** were grown from a saturated acetonitrile solution; the molecular structure of the complex is shown in Figure 1.

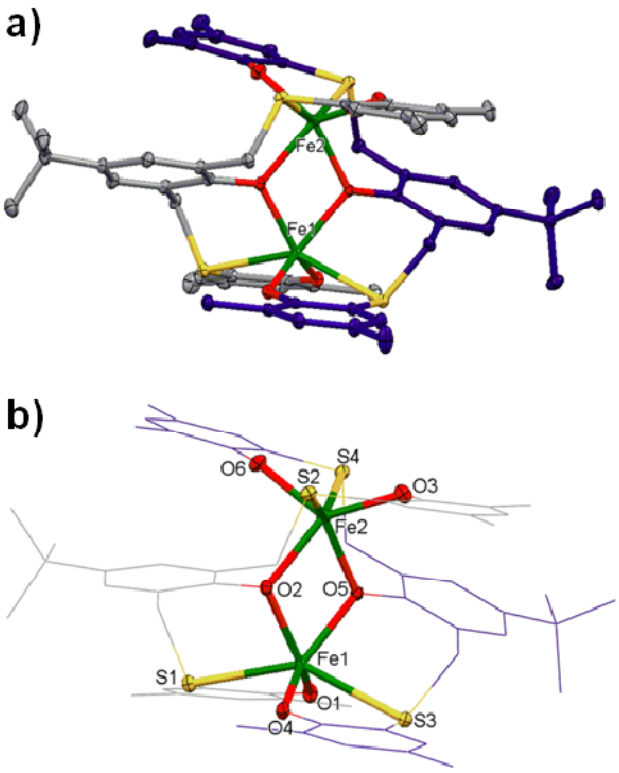

Figure 1. Molecular structure of complex **6**. a) the structure is shown for the sake of clarity with the C atoms of one of the two ligands represented in violet color (hydrogen atoms have been omitted). Selected bond lengths (Å): Fe(1)•••Fe(2) 3.331; Fe(1)-O(1) 1.8894(14); Fe(1)-O(4) 1.9030(13) Fe(1)-O(5) 2.0314(13); Fe(1)-O(2) 2.0384(14); Fe(1)-S(1) 2.6102(5); Fe(1)-S(3) 2.6466(5); Fe(2)-O(6) 1.8943(14); Fe(2)-O(3) 1.8994(15); Fe(2)-O(5) 2.0345(13); Fe(2)-O(2)

Published as Adv. Synth. Catal. 2016, 358, 3231-3243. doi.org/10.1002/adsc.201600621

2.0514(14); Fe(2)-S(2) 2.5914(5); Fe(2)-S(4) 2.6585(5). b) the coordination geometry of the two iron (III) centers is highlighted.

It is worth noting that each ligand is coordinated to both iron atoms with the central phenolate moiety bridging the metal centers presumably to relieve steric strain of the ligand. The molecule adopts an idealized D_2 symmetry being one axis coincident with the Fe-Fe vector. Each iron(III) in the dimeric complex exhibits six-coordinated $[O_4S_2]$ environment generated by four phenoxo oxygens and two sulfur atoms. The Fe-O(bridging) bond lengths in **6** are longer than the Fe-O(non bridging) ones. These Fe-O distances are slightly longer, for example, than the corresponding ones found in an iron(III)tiocalix[4]arene complex[27] . The Fe-S interactions are rather weak and fall in the range 2.5914-2.6585(5) Å whereas the Fe-Fe distance of 3.331 Å indicates that no bonding interaction is present.

Cycloaddition of CO_2 to epoxides promoted by catalysts 1-6

Aiming to optimize the reaction parameters in the cycloaddition of CO_2 to (±)-propylene oxide (PO) we used the complex **6** as benchmark under solvent-free conditions. A screening of various co-catalyst, namely dimethylaminopyridine (DMAP), bis(triphenylphosphine)iminium chloride (PPNCl) or quaternary ammonium salts such as tetrabutylammonium chloride (TBAC), iodide (TBAI) and bromide (TBAB) in combination with 0,5 equivalent of **6** (0.025 *mol%*) was performed (see Figure 2a, entries **S1-5** of Table S1 in the supporting information). Notably, by varying the amount of TBAB from 0.05 *mol*% to 0.25 mol% an appreciable improvement of the catalytic activity is observed (entries **S5-7**, Table S1). Increasing the temperature from 80 to 140 °C, results in a linear increasing of the TOF (Figure 2b; entries **S5** and **S8-10** of Table S1).

Published as Adv. Synth. Catal. 2016, 358, 3231-3243. doi.org/10.1002/adsc.201600621

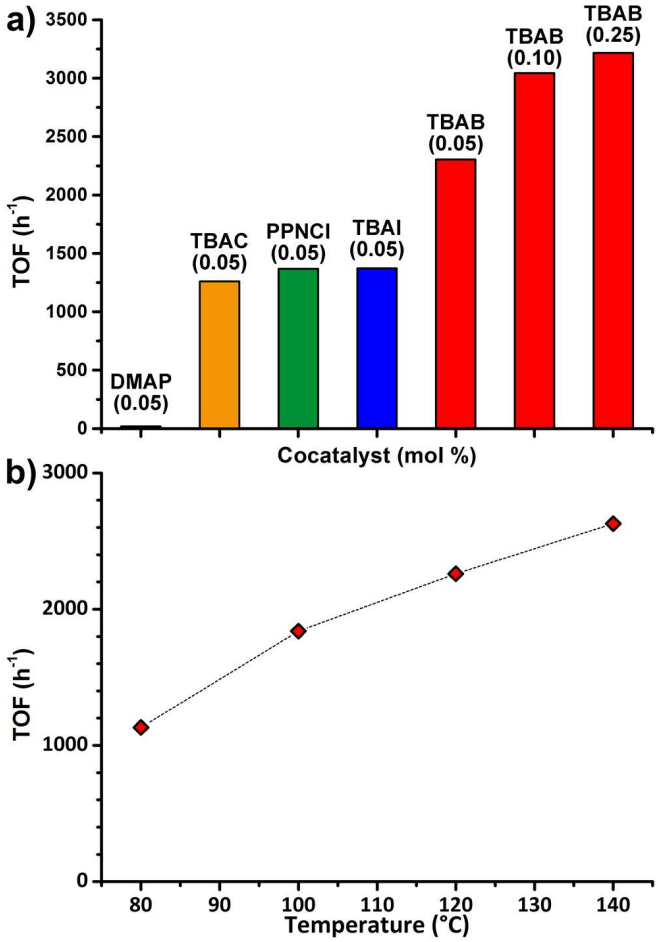

Figure 2. Effect of the co-catalyst type and loading (a) and of temperature (b) on the catalytic activity of **6** in PO/CO_2 coupling.

A control experiment using TBAB without the iron complex results in very low conversion (10%; entry **S11**, Table S1), compared to the binary system under the same reaction conditions (80%; entry **S7**, Table S1). The effect of the CO_2 pressure on the catalytic activity was also investigated (compare entries **S12-14**, Table S1); by reduction of the pressure from 2.0 to 0.5 MPa the activity does not drop dramatically, while by increasing the pressure to 4.0 MPa an activity enhancement from 3300 to 4000 h^{-1}, reaching complete conversion of PO in only 1 hour,

Published as Adv. Synth. Catal. 2016, 358, 3231-3243. doi.org/10.1002/adsc.201600621

was observed. Owing to these good results the catalyst loading was reduced from 0.025 to 0.01 *mol%*, in order to compare the catalytic activity of complexes **1-6** in the coupling of CO_2 with PO (Table 1).

Table 1. CO_2/propylene oxide coupling promoted by the Iron(III) complexes **1-6**.

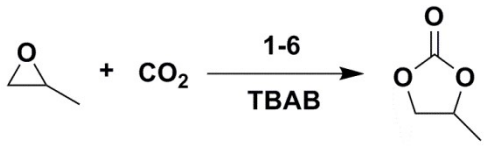

Entry[a]	Catalyst	Conversion[b,c] (*mol%*)	TOF[d] h^{-1}
1	**1**	43.0	4300
2	**2**	35.5	3550
3	**3**	40.4	4040
4	**4**	36.3	3630
5	**5**	50.0	4990
6	**6**	52.0	5200
7[e]	-	5	-

[a] Reaction conditions: PO = 5 mL, 7.15×10^{-2} mol; Catalyst = 1.43×10^{-5} mol (0.01 *mol%*); TBAB = 1.43×10^{-4} mol (0.1 *mol%*); PO/TBAB/Catalyst = 10000/10/1; T = 120 °C; P_{CO2} = 2.0 MPa; reaction time = 1 h. [b] Determined by ^{1}H NMR using mesitylene as internal standard. [c] The selectivity toward the formation of PC was always found to be >99%. [d] Turnover frequency ($mol_{PC} \times mol_{Catalyst}^{-1} \times$ reaction time^{-1}). [e] Control experiment in absence of the iron catalyst.

The best performance was achieved using complex **6**, with a TOF equal to 5200 h^{-1} under relatively mild reaction conditions (entry 6, Table 1). To the best of our knowledge, this is the highest TOF for an iron based catalyst reported in literature and not far from those observed for

Published as Adv. Synth. Catal. 2016, 358, 3231-3243. doi.org/10.1002/adsc.201600621

the most active catalysts based on magnesium or aluminum.[2d] Complex **5** also showed to be highly active, with conversion near to that of **6** (compare entries 5 and 6, Table 1), suggesting that the electronic effect of the substituent $\mathbf{R_2}$ does not play a relevant role in the determination of the catalytic performance. On the other hand, the introduction of chlorine atoms in the $\mathbf{R_1}$ positions, as in complex **4**, has a deleterious effect on the catalytic activity (compare entries 4 and 6, Table 1). In addition, the appreciable lower activity displayed by complex **2**, bearing the more steric demanding cumyl groups on the phenol rings, confirms that the catalytic activity is strongly influenced by the bulkiness of the substituents of the external phenol rings.

Table 2. CO_2/hexene oxide coupling promoted by Iron(III) complexes **1-6**.

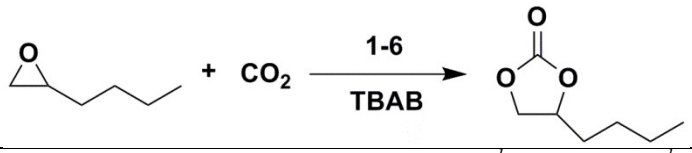

Entry[a]	Catalyst	Conversion[b,c] (*mol%*)	TOF[d] (h^{-1})
8	**1**	45.7	2290
9	**2**	17.9	900
10	**3**	43.1	2160
11	**4**	35.0	1750
12	**5**	67.8	3390
13	**6**	68.9	3450

[a] Reaction conditions: hexene oxide = 8.6 mL, 7.15×10^{-2} mol; Complex = 1.43×10^{-5} mol; TBAB = 1.43×10^{-4} mol; T = 120 °C; P_{CO2} = 4.0 MPa; reaction time = 1 h. [b] Determined by ^{1}H-NMR using mesitylene as internal standard. [c] The selectivity toward the formation of hexene carbonate (HC) was always found to be >99%. [d] Turnover frequency ($mol_{HC} \times mol_{Catalyst}^{-1} \times$ reaction time^{-1}).

Published as Adv. Synth. Catal. 2016, 358, 3231-3243. doi.org/10.1002/adsc.201600621

To further evaluate the role of the steric demand around the catalytic site on the catalytic performance, the coupling of CO_2 with a bulkier terminal epoxide such as the 1,2-epoxyhexane was performed (Table 2). Both **5** and **6** exhibit again the highest activities (respectively 3390 and 3450 h^{-1}), with differences in the order of the experimental error (entries 12-13, Table 2). Notably, the longer alkyl chain on the epoxide ring exalts differences in the activity due to the steric hindrance of the substituents in the $\mathbf{R_1}$ positions, with complex **2** displaying a considerably lower activity (entry 9, Table 2). The less steric demanding complex **3** shows lower activity compared to **6** due to solubility issue in the reaction medium as previously reported.[11b]

In order to investigate the applicability of the catalytic system **6**/TBAB to a wider range of substrates, we performed the coupling reaction of carbon dioxide with a series of mono-, di-substituted and internal epoxides. The results summarized in the Table 3 clearly show that the presence of an electron withdrawing substituent in the substrate, such as a chlorine atom in epichlorohydrin, has a positive effect with a TOF of 7000 h^{-1} (entry 14, Table 3). Conversely, the presence of an electron releasing group, such as a phenoxy or a phenyl group results in a attenuation of the reactivity (entries 15-17, Table 3). Notably the more challenging substrate isobutylene oxide (1,1-dimethyloxirane) was converted in good yield to the corresponding carbonate (entry 19 of Table 3). Moreover the *cis* form of 1,2-dimethyloxirane was converted to the corresponding carbonate not only in good yield but also with a high degree of configuration retention (entry 20, Table 3).

Published as Adv. Synth. Catal. 2016, 358, 3231-3243. doi.org/10.1002/adsc.201600621

Table 3. CO_2/Epoxide coupling promoted by Iron(III) complexes **6**.

Entry[a]	Substrate	Epoxide/ TBAB/**6** (molar ratio)	Product	Conversion[b,c] (*mol%*)	*cis*:*trans*[d] (molar ratio)	TOF[e] h^{-1}
14	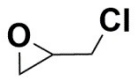	10000/10/1	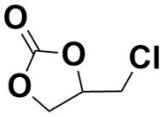	70.0	-	7000
15	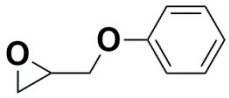	10000/10/1	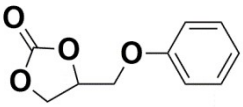	44.5	-	4450
16	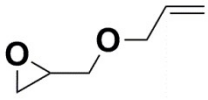	10000/10/1	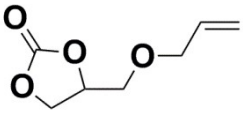	21.0	-	2100
17	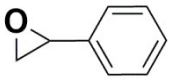	10000/10/1	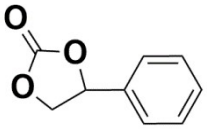	13.0	-	1300
18[f]	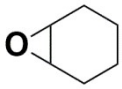	1000/10/1	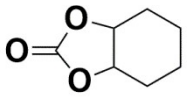	55.0	>99:1	550
19[f, g]		1000/10/1	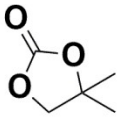	65.8	-	660
20[f, g]		1000/10/1	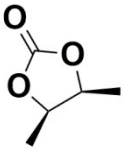	67.1	97:3	670
21[f, g]		1000/2/1	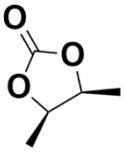	12.6	98:2	125
22[g, h]	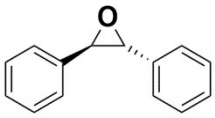	1000/10/1	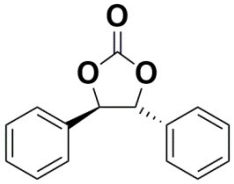	7.3	>1:99	70

[a] Reaction conditions: epoxide = 7.15×10^{-2} mol; T = 120 °C; P_{CO2} = 2.0 MPa; reaction time = 1 h. [b] Determined by ^{1}H NMR using mesitylene as internal standard. [c] The selectivity toward the formation of cyclic carbonate was always found >99%. [d] Determined by ^{1}H NMR [e] Turnover Frequency ($mol_{Carbonate} \times mol_{Catalyst}^{-1} \times$ reaction $time^{-1}$). [f] Epoxide = 1.0 mL. [g] P_{CO2} = 4.0 MPa. [h] Stilbene oxide = 1.0 g, MEK = 2.0 mL.

Published as Adv. Synth. Catal. 2016, 358, 3231-3243. doi.org/10.1002/adsc.201600621

Intriguingly, complex **6** in combination with TBAB retains the configuration of the starting substrate regardless of the cocatalyst/catalyst molar ratio (compare entries 20 and 21, Table 3) indicating that the attack of the bromide anion to the epoxide ring proceeds selectively via two consecutive inversion of configuration (**S_N2**) on the same stereocenter and that, differently to what reported for other iron(III) based catalyst,[10f] this mechanism is not dependent on the bromide concentration. (See Scheme 2).

Scheme 2. Proposed mechanism for the retention of stereochemical configuration in the production of cis-4,5-dimethyl-1,3-dioxolan-2-one from cis-2,3-epoxybutane and CO_2 promoted by catalyst **6** in presence of TBAB.

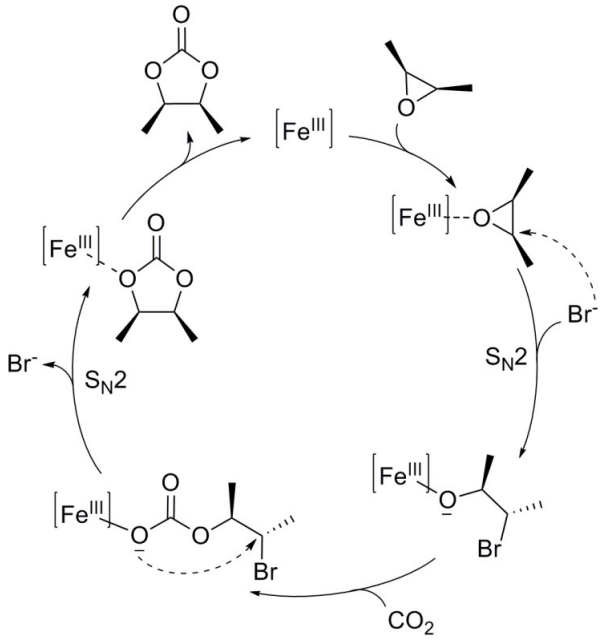

A complete stereoretention was also observed in the case of *trans*-stilbene oxide (entry 22, Table3) and the exclusive formation of *cis*-cyclohexenecarbonate (*cis*-CHC) (entry 18, Table3)

Published as Adv. Synth. Catal. 2016, 358, 3231-3243. doi.org/10.1002/adsc.201600621

also support the proposed reaction mechanism. In fact, the thermodynamically disfavored formation of *cis*-CHC should necessary arise from a mechanism involving a double inversion of the starting CHO configuration. [2d]

Theoretical Calculations

Deeper insights into the reaction mechanism were obtained by performing DFT on the reaction mechanism for the cycloaddition of CO_2 to PO catalyzed by complex **6** in presence of TBAB, the complete energy profile is reported in Figure 3 (for clarity, we refer to the two Fe(III) centers in **6** as Fe_1 and Fe_2).

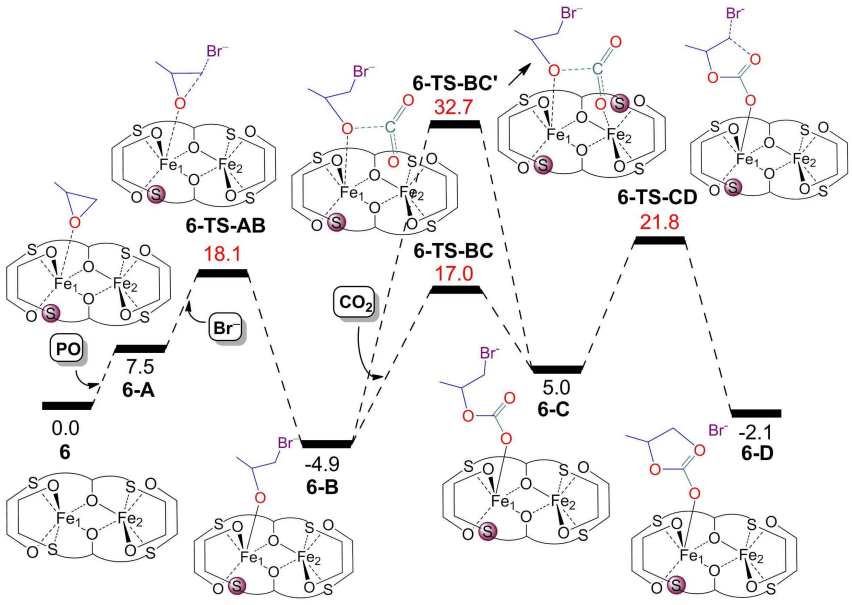

Figure 3. Computed free energy surface for the cycloaddition of propylene oxide (PO) and CO_2 catalyzed by species **6**/TBAB. The free energies in solution (PO as the solvent) are given in kcal/mol relative to the starting complex **6**. The energy values in red represent the energies of the transition states. ● indicates decoordination of a hemilabile S atom.

Published as Adv. Synth. Catal. 2016, 358, 3231-3243. doi.org/10.1002/adsc.201600621

Coordination of PO to the Fe_1 center in **6** is only possible by dissociation one of the two hemilabile S atoms (r(Fe_1-S) 2.704 Å). PO coordination is calculated to be endergonic and leads to intermediate **6-A**, which lies 7.5 kcal/mol above **6**. From a structural point of view, in **6-A** PO coordinates to the Fe_1 center (r(Fe_1-O) = 2.412 Å) in the coordination position previously occupied by the dissociated S atom. PO coordination results in a slight decrease in the Fe_1-Fe_2 distance in **6-A** when compared to the catalyst species **6** (3.271 vs 3.364 Å, respectively; see Figure 4).

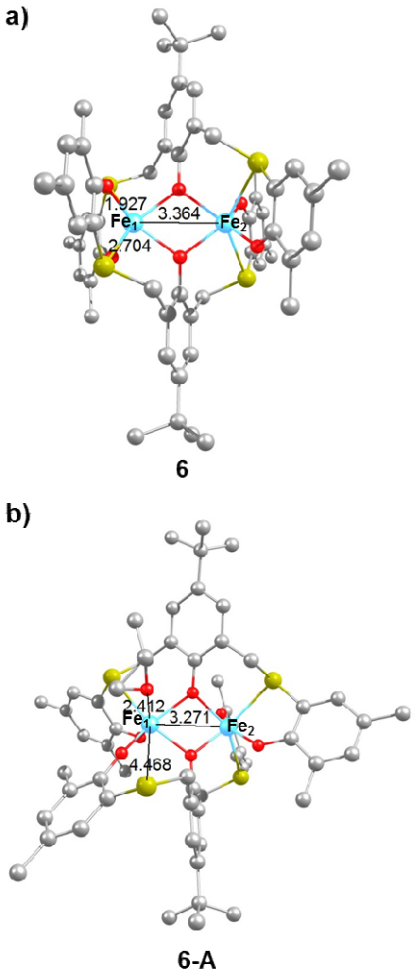

Figure 4. Geometry of the starting complex **6** (a) and of the PO coordinated intermediate **6-A** (b). Hydrogen atoms omitted for clarity and the selected distances in Å.

Published as Adv. Synth. Catal. 2016, 358, 3231-3243. doi.org/10.1002/adsc.201600621

To explore the eventual dissociation of one of the two Fe_1-S bonds prior to PO coordination in the starting complex **6**, we removed PO from the optimized geometry of intermediate **6-A** and we re-optimized the complex. The resulting complex with Fe_1-S bond being dissociated is lying only 5.8 kcal/mol above species **6**, in line with the expected lability of the S binding. The experimental evidence that the introduction of the electron withdrawing chlorine atoms on the lateral phenol rings (complex **4**) results in a lowering of the catalytic activity supports this scenario. As a matter of fact, the coordinating ability of the phenoxide O atoms should be reduced in **4** due to the presence of the *ortho* Cl atom. This should result in increased Lewis acidity at the metal center and should reduce the lability of the sulfur atoms, rendering substitution of one sulphur moiety by PO less favorable. This scenario is supported by our calculations on complex **4**, which presents slightly shorter Fe_1-S distances when compared to complex **6** (2.66 Å vs 2.70 Å, see Figure S1). Consistently, dissociation of one Fe_1-S bond from complex **4** requires 8.6 kcal/mol versus 5.8 kcal/mol in **6**, and the PO coordinated intermediate **4-A**, is slightly less stable than **6-A** (8.7 vs 7.5 kcal/mol).

Back to the main mechanism catalyzed by **6**, the next step from the PO coordinated specie **6-A** corresponds to the opening of the PO ring by a Br anion, leading to the formation of the more stable intermediate **6-B**, 5.5 kcal/mol below **6**. This step proceeds through transition state **6-TS-AB** and requires overcoming an overall barrier of 18.1 kcal/mol above **6**. Then, we studied insertion of CO_2 into the Fe-O bond in the intermediate **6-B** to give the hemicarbonate intermediate **6-C**, which lies 10.0 kcal/mol above **6-B**. This CO_2 insertion step requires the overcoming of a barrier (**6-TS-BC**) of 21.9 kcal/mol from the most stable intermediate **6-B**. To our surprise, despite the relatively low calculated barrier we did not observe any cooperativity

Published as Adv. Synth. Catal. 2016, 358, 3231-3243. doi.org/10.1002/adsc.201600621

between the two Fe centers, since the CO_2 molecule is quite away from the Fe_2 center (r(Fe_2-CO_2) = 3.772 Å), see Figure 5a.

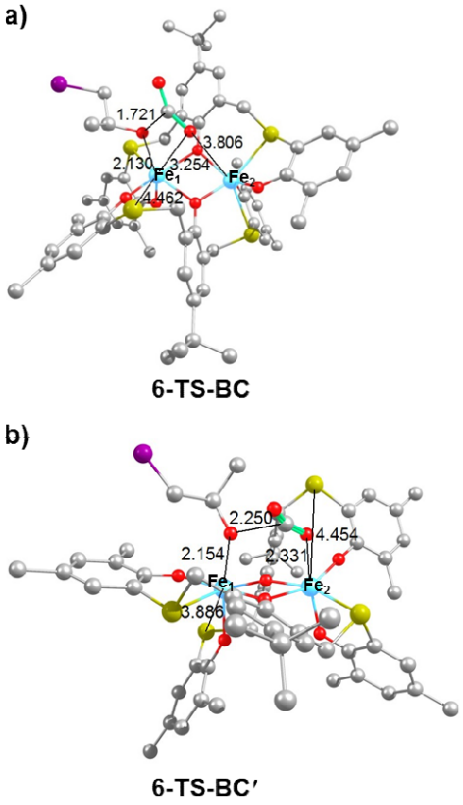

Figure 5. Geometry of transition states **6-TS-BC** (a) **6-TS-BC'** (b), for insertion of CO_2 into the Fe-O bond. Hydrogen atoms omitted for clarity and the selected distances in Å.

As a further check on the possible cooperativity between the two Fe centers in the CO_2 insertion step, we calculated an alternative transition state for CO_2 insertion, **6-TS-BC'**, by forcing decoordination of one of the two hemilabile S atoms from the Fe_2 center. In this case we observed a clear interaction between the Fe_2 center and one of the O atoms of the CO_2 molecule (r(Fe_2-CO_2) = 2.320 Å), see Figure 5b. However, transition state **6-TS-BC'** is placed 15.7

Published as Adv. Synth. Catal. 2016, 358, 3231-3243. doi.org/10.1002/adsc.201600621

kcal/mol higher in energy relative to transition state **6-TS-BC**. These observations suggest that though the catalyst species **6** under investigation is bimetallic, catalysis essentially occurs at a single Fe(III) center without cooperation of the second Fe(III) center. This is clearly different from the case of PO coupling with CO_2 to cyclic carbonate promoted by mono-metallic Nb complexes, where cooperativity between two Nb centers occurs both in the homogeneous phase as well as after grafting of the Nb complex on silica.[28] Next, starting from intermediate **6-C**, we studied the ring closing step leading to the formation of intermediate **6-D** with the desired cyclic carbonate product coordinated to the Fe metal center. According to calculations, ring closing is predicted to be the rate determining step, with a barrier of 26.7 kcal/mol (**6-TS-CD**) relative to the most stable intermediate **6-B**. This is clearly a high barrier, which is however consistent with the remarkably high temperature of 120 °C needed experimentally to achieve a yield of at least 51% in 1 hour. Finally, intermediate **6-D** would release the carbonate product and a Br^- anion, regenerating intermediate **6-A** with recoordination of a free PO molecule, thus closing the catalytic cycle.

CONCLUSIONS

We have reported the synthesis and the complete characterization of three novel bimetallic iron(III) complexes (**4-6**) bearing thioether-triphenolate ligands. When activated by tetrabutylammonium bromide the title iron(III) complexes result very effective in the cycloaddition of CO_2 to epoxides giving the highest initial activity so far reported for an iron based catalyst. In particular, complex **6** shows the best catalytic performance in terms of activity and selectivity for several terminal epoxides with TOF values up to 5200 h^{-1} for the conversion

Published as Adv. Synth. Catal. 2016, 358, 3231-3243. doi.org/10.1002/adsc.201600621

of PO to PC. Furthermore complex **6** also promotes the conversion to the corresponding cyclic carbonates of internal epoxides with a high degree of stereocontrol in the ring-closing reaction, leading to the retention of configuration of the starting epoxide (≥97%) via a mechanism involving a double inversion of the initial epoxide configuration. Finally the mechanistic studies show that in spite of the dinuclear nature of the catalyst precursor only one metal center is operative in the catalytic cycle and that coordination of the substrate and the subsequent reaction pathway can only take place by dissociation of a hemilabile S atom from one of the iron centers. These findings not only show that is possible to obtain highly active catalytic systems based on iron(III) for the CO_2/epoxides coupling but also highlight the fundamental role of this sulfur containing ligands in modulating the Lewis acidity of the iron center and thus the reactivity with CO_2 and oxiranes for this family of catalysts.

ASSOCIATED CONTENT

Supporting Information

Further experimental details, NMR, MS, UV-vis, FT-IR spectroscopic characterizations, Crystallographic data, Cartesian coordinates of the DFT optimized geometries, complete ref. 18. This material is available free of charge via the Internet at http://pubs.acs.org.

AUTHOR INFORMATION

Corresponding Author

* E-mail for C.C.: ccapacchione@unisa.it

Published as Adv. Synth. Catal. 2016, 358, 3231-3243. doi.org/10.1002/adsc.201600621

* E-mail for L.C.: luigi.cavallo@kaust.edu.sa

Author Contributions

C.C., F.D.M., A.B., S.M. and A.G. have designed the catalytic systems and realized the experiments; M.M. and A.D.N. have performed the structural resolution by x-ray diffraction of the catalyst; L.C. and S.V.C.V. have performed the DFT calculations. The manuscript was written through contributions of all authors. All authors have given approval to the final version of the manuscript.

Funding Sources

Financial support is acknowledged from the Ministero dell'Istruzione dell'Università e della Ricerca (MIUR, Roma, Italy for FARB 2015) and the SPRING cluster (REBIOCHEM research project CTN01_00063_49393).

ACKNOWLEDGMENT

The Centro di Tecnologie Integrate per la Salute (Project PONa3_00138) for the 600 MHz NMR instrumental time is acknowledged. The authors are also grateful to Dr. Guglielmo Monaco from University of Salerno for useful discussion, Dr. Patrizia Oliva and Dr. Patrizia Iannece from University of Salerno for technical assistance. LC acknowledges the King Abdullah University of Science and Technology for supporting this research.

ABBREVIATIONS

CHC, cyclohexene carbonate; CHO, cyclohexene oxide; DMAP, dimethylaminopyridine; HC, hexene carbonate; HO, hexene oxide; PC, propylene carbonate; PO, propylene oxide; PPNCl,

Published as Adv. Synth. Catal. 2016, 358, 3231-3243. doi.org/10.1002/adsc.201600621

bis(triphenylphosphine)iminium chloride; TBAB, tetrabutylammonium bromide; TBAC, tetrabutylammonium chloride; TBAI, tetrabutylammonium iodide.

REFERENCES

(1) (a) Qiao, J., Liu, Y.; Hong, Y.; Zhang, *J. Chem. Soc. Rev*. **2014**, *43*, 631-675. (b) Maeda, C.; Miyazaki, Y.; Ema, T. *Catal. Sci. Technol*. **2014**, *4*, 93-99. (c) Aresta, M.; Dibenedetto, A.; Angelini, A. *Chem. Rev*., **2013**, *114*, 1709–1742. (d) Omae, I. *Coord. Chem. Rev*., **2012**, *256*, 1384–140. (e) Cokoja, M.;Bruckmeier, C.; Rieger, B.; Herrmann, W. A.; Kuhn, F. E. *Angew. Chem., Int. Ed*. **2011**, *50*, 8510−8537. (f) Quadrelli, E.A.; Centi, G.; Duplan, J.-L., Perathoner, S. *ChemSusChem*, **2011**, *4*, 1194–1215; (g) Darensbourg, D. J. *Inorg. Chem*., **2010**, *49*, 10765–10780 (h) Aresta, M.; Dibenedetto, A. *Dalton Trans*., **2007**, 2975–2992; (i) Sakakura, Y.; Choi, J.-C.; Yasuda, H. *Chem. Rev*. **2007**, *107*, 2365−2387 (l) Activation of Carbon Dioxide, ed. S. L. Suib, *Elsevier*, Amsterdam, **2013**.

(2) (a) Whiteoak, C. J.; Kleij, A. W. *Synlett* **2013**, *24*, 1748−1756. (b) North, M.; Pasquale, R.; Young, C. *Green Chem*. **2010**, *12*, 1514−1539. (c) Decortes, A.; Castilla, A. M.; Kleij, A. W. *Angew. Chem., Int. Ed*. **2010**, *49*, 9822−9837. (d) Martin, C.; Fiorani, G.; Kleij, A. W. *ACS Catal*. **2015**, *5*, 1353−1370. (e) Comerford, J. W.; Ingram, I. D.; North, M.; Wu, X. *Green Chem*. **2015**, *17*, 1966−1987.

(3) (a) Lu, X.-B.; Darensbourg, D.J. *Chem. Soc. Rev*. **2012**, *41*, 1462–1484. (b) Darensbourg, D.J.; Wilson, S.J. *Green Chem*. **2012**, *14*, 2665−2671. (c) Lu, X.-B.; Ren, W._M.; Wu, G.-P. *Acc. Chem. Res*. **2012**, *45*, 1721–1735. (d) Klaus, S.; Lehenmeier, M.W.; Anderson, C.E.; Rieger, B. *Coord. Chem Rev*., **2011**, *255*, 1460-1479. (e) Kember, M.R.; Buchard, A.; Williams

Published as Adv. Synth. Catal. 2016, 358, 3231-3243. doi.org/10.1002/adsc.201600621

C.K. *Chem. Commun*. **2011**, *47*, 141–163. (f) Darensbourg, D.J. *Chem. Rev*., **2007**, *107*, 2388–2410. (g) Coates, G.W.; Moore, D.V. *Angew. Chem., Int. Ed*. **2004**, *43*, 6618−6639.

(4) (a) Element Recovery and Sustainability (RSC Green Chemistry series vol. 22), (Ed.: A. J. Hunt), RSC Publishing, Cambridge, **2013**.(b) R. M. Izatt, S. R. Izatt, R. L. Bruening, N. E. Izatta, B. A. Moyer, *Chem. Soc. Rev*. **2014**, *43*, 2451–2475.

(5) (a) Liu, X.F.; Song, Q.W.; Zhang, S.; He, L.N. *Catal. Today* **2016**, *263*, 69-74. (b) Cokoja, M.; Wilhelm, M.E.; M.H. Anthofer, M.H.; Hermann, W.A. ; Kühn, F.E. *ChemSusChem* **2015**, *8*, 2436-2454. (c) Fiorani, G.; Guo, W. ; Kleji, A.W. *Green Chem*., **2015**, *17*, 1375-1389. (d) He, Q.; O'Brien, J. W.¸. Kitselman, K. A.; Tompkins, L. E.; Curtis and, G. C. T.; Kerton, F. M. *Catal. Sci. Technol*., **2014**, *4*, 1513–1528. (e) Li, H.; Bhadury, P. S.; Song, B.; Yang, S. *RSC Advances*, **2012**, *2*, 12525–12551. (f) Yang, Z.–Z.; Zhao, Y.–N. He, L.–N. *RSC Advances*, **2011**, *1*, 545–567.

(6) (a) Lu, X.–B .; Zhang, Y.–J.; Jin, K.; Luo, L.–M.;.Wang, H. *J. Catal*., **2004**, *227*, 537–541. (b) Tian, D.; Liu, B.; Gan, Q .; Li, H.; Darensbourg, D.J. *ACS Catal*., **2012**, *2*, 2029–2035. (c) (Castro-Osma, J. A.; Alonso-Moreno, C.; Lara-Sánchez, A.; Martinez, J.; North, M.; Otero, A. *Catal. Sci. Technol*. **2014**, *4*, 1674−1684. (d) Martínez, J.; Castro-Osma, J.A.; Earlam, A.; Alonso-Moreno, C.; Otero, A.; Lara-Sánchez, A.; North, M.; Rodríguez-Diéguez, A. . *Chem. Eur. J*., **2015**, *21*, 9850-9862. (e) North, M.; Quek, S.C.Z.; Pridmore, N.E.; Whitwood, A.C.; Wu, X. *ACS Catal*., **2015**, *5*, 3398-3402. (f) Castro-Osma, J. A.; North, M.; Wu, X. *Chem. Eur. J*., **2016**, *22*, 2100-2107. (g) Kim, S. H.; Ahn, D.; Go, M. J.; Park, M. H.; Kim, M.; Lee, J.; Kim, Y. *Organometallics* **2014**, *33*, 2770−2775. (h) Cozzolino, M.; Press, K.; Mazzeo, M.; Lamberti, M. *ChemCatChem* **2016**, *8*, 455-460. (i) Supasitmongkol, S.; Styring, P. *Catal. Sci. Technol.*

2014, *4*, 1622–1630. (j) Ren, Y.; Jiang, O.; Mao, Q.; Jiang, H. *RSC Advances*, **2016**, *6*, 3243-3249. (k) Fuchs, M. A.; Altesleben, C.; Zevaco T. A .; Dinjus, E. *Eur. J. Inorg. Chem*., **2013**, 4541–4545.

(7) (a) Meléndez, J.; North, M.; Villuendas, P. *Chem. Commun*. **2009**, 2577−2579. (b) Clegg, W.; Harrington, R. W.; North, M.; Pasquale, R. *Chem. -Eur. J*. **2010**, *16*, 6828−6843. (c) North, M.; Young, C. *Catal. Sci. Technol*. **2011**, *1*, 93−99. (d) Beattie, C.; North, M.; Villuendas, P.; Young, C. *J. Org. Chem*. **2013**, *78*, 419−426. (e) Castro-Osma, J. A.; Lara-Sanchez, A.; North, M.; Otero, A.; Villuendas, P. *Catal. Sci. Technol*. **2012**, *2*, 1021−1026. (f) Castro-Osma, J. A.; North, M.; Wu, X. *Chem. Eur. J*., **2014**, *20*, 15005–15008. (g) North, M.; Quek, S.C.Z.; Pridmore, N.E.; Whitwood, A.C.; Wu, X. *ACS Catal*., **2015**, *5*, 3398-3402. (h) North, M.; Wang, B.;Young, C. *Energy Environ. Sci*. **2011**, *4*, 4163−4170. (i) Melendez, J.; North, M.; Villuendas, P.; Young, C. *Dalton Trans*. **2011**, *40*, 3885− 3902. (j) North, M.; Young, C. *Catal. Sci. Technol*. **2011**, *1*, 93−99. (k) Clegg, W.; Harrington, R. W.; North, M.; Villuendas, P. *J. Org. Chem*. **2010**, *75*, 6201−6207. (l) North, M.; Villuendas, P.; Young, C. *Chem. Eur. J*. **2009**, *15*, 11454−11457. (m) North, M.; Pasquale, R. *Angew. Chem., Int. Ed*. **2009**, *48*, 2946−2948. (n) Melendez, J.; North, M.; Pasquale, R. *Eur. J. Inorg. Chem*. **2007**, 3323−3326.

(8) (a) Whiteoak, C. J.; Kielland, N.; Laserna, V.; Escudero–Adán, E. C.; Martin, E.¸ Kleij, A.W. *J. Am. Chem. Soc*., **2013**, *135*, 1228–1231. (b) Whiteoak, C. J.; Kielland, N.; Laserna, V.; Castro–Gómez, F.; Martin, E.; Escudero–Adán, E.C.; Bo, C.; Kleij, A. W. *Chem. Eur. J*., **2014**, *20*, 2264–2275. (c) Rintjema, J.; Guo, W.; Martin, E., Escudero-Adán, E.C.; Kleij, A.W. *Chem. Eur. J*., **2015**, *21*, 10754-10762.

Published as Adv. Synth. Catal. 2016, 358, 3231-3243. doi.org/10.1002/adsc.201600621

(9) (a) Bauer, I.; Knölker, H.-J. *Chem. Rev*. **2015**, *1151*, 3170–3387. (b) Sun, C.-L.; Li, B.-J.; Shi, Z.-J. *Chem. Rev*. **2011**, *111*, 1293-1314. (c) Correa, A.; García Mancheño, O.; Bolm, C. *Chem. Soc. Rev*. **2008**, *37*, 1108-1137. (d) Bolm, C.; Legros, J.; Le Paih, J.; Zani, L. *Chem. Rev*. **2004**, *104*, 6217-6254.

(10) (a) Taherimehr, M.;. Sertã, J. P. C. C.; Kleij, A. W.; Whiteoak, C. J.; Pescarmona, P.P. *ChemSusChem*, **2015**, *8*, 1034-1042. (b) Sheng, X.; Qiao, L.; Qin, Y.; Wang, X.; Wang, F. *Polyhedron*, **2014**, *74*, 129-133. (c) Adolph, M.; Zevaco, T. A.; Altesleben, C.; Walter and, O.; Dinjus, E. *Dalton Trans*., **2014**, *43*, 3285–3296; (d) Fuchs, M. A.; Zevaco, T. A.; Ember, E.; Walter, O.; Held, I.; Dinjus, E.; Doring, M. *Dalton Trans*., **2013**, *42*, 5322–5329; (e) Taherimehr, M.; Al-Amsyar, S. M.; Whiteoak, C. J.; Kleij, A. W.; Pescarmona, P.P. *Green Chem*., **2013**, *15*, 3083–3090; (f) Whiteoak, C. J.; Martin, E.; Escudero-Adán, E.; Kleij, A. W. *Adv. Synth. Catal*., **2013**, *355*, 2233–2239; (g) Whiteoak, C. J.; Martin, E.; Belmonte, M. M.; Benet-Buchholz, J.; Kleij, A. W. *Adv. Synth. Catal*., **2012**, *354*, 469–476; (h) Whiteoak, C. J.; Gjoka, B.; Martin, E.; Belmonte, M. M.; Escudero-Adán, E. C.; Zonta, C.; Licini, G.; Kleij, A. W. *Inorg. Chem*. **2012**, *51*, 10639–10649; (i) Buchard, A.; Kember, M. R.; Sandeman, K. G.; Williams, C. K. *Chem. Commun*., **2011**, *47*, 212–214; (j) Dengler, J. E. ; Lehenmeier, M. W.; Klaus, S.; Anderson, C. E.; Herdtweck, E.; Rieger, B. *Eur. J. Inorg. Chem*. **2011**, 336–343.

(11) (a) Buonerba, A.; Della Monica, F.; De Nisi, A.; Luciano, E.; Milione, S.; Grassi, A.; Capacchione, C.; Rieger, B., Thioether-triphenolate bimetallic iron(iii) complexes as robust and highly efficient catalysts for cycloaddition of carbon dioxide to epoxides. *Faraday Discuss*. **2015**, *183* (0), 83-95; (b) Buonerba, A.; De Nisi, A.; Grassi, A.; Milione, S.; Capacchione, C.; Vagin, S.; Rieger, B. *Catal. Sci. Technol*. **2015**, *5*, 118−123.

Published as Adv. Synth. Catal. 2016, 358, 3231-3243. doi.org/10.1002/adsc.201600621

(12) (a) Evans, D. F.; *J. Chem. Soc*., **1959**, 2003-2005; (b) J. L. Deutsch, S. M. Poling; *J. Chem. Ed*., **1969**, *46*, 167-168; (c) Physical Methods in Bioinorganic Chemistry, ed. Lawrence Que Jr., University Science Books, Sausalito, CA, **2000**.

(13) (a) Morris, B. L.; Wold, A. *Review of Scientific Instruments*, **1968**, *39*, 1937-1941; (b) Lindoy, L. F.; Katović, V; Busch, D. H.; *J. Chem. Educ*., **1972**, *49*, 117-120.

(14) *SMART & SAINT Software Reference Manuals*, version 5.051 (Windows NT Version), Bruker Analytical X-ray Instruments Inc.: Madison, WI, **1998**.

(15) G. M. Sheldrick, *SADABS*, program for empirical absorption correction, University of Göttingen, Germany, **1996**.

(16) M. C. Burla, R. Caliandro, M. Camalli, B. Carrozzini, Cascarano, G. L. De Caro, C. Giacovazzo, G. Polidori, R. Spagna, *J. Appl. Crystallogr*. **2005**, *38*, 381-388.

(17) G. M. Sheldrick, SHELXTL*plus* (Windows NT Version) Structure Determination Package, Version 5.1. Bruker Analytical X-ray Instruments Inc.: Madison, WI, USA, **1998**.

(18) (a) Frisch, M. J. et al. Gaussian 09 Revision A.1, Gaussian, Inc., Wallingford, CT, **2009**.

(19) (a) Becke, A. D. *Phys. Rev. A* **1988**, *38*, 3098-3100. (b) Perdew, J. P. *Phys. Rev. B*, **1986**, *33*, 8822-8824. (c) Perdew, J. *P. Phys. Rev. B* **1986**, *34*, 7406-7406.

(20) Schaefer, A.; Horn, H.; Ahlrichs, R. *J. Chem. Phys*. **1992**, *97*, 2571-2577.

(21) (a) Haeusermann, U.; Dolg, M.; Stoll, H.; Preuss, H. *Mol. Phys*. **1993**, *78*, 1211-1224. (b) Kuechle, W.; Dolg, M.; Stoll, H.; Preuss, H. *J. Chem. Phys*. **1994**, *100*, 7535-7542. (c) Leininger, T.; Nicklass, A.; Stoll, H.; Dolg, M.; Schwerdtfeger, P. *J. Chem. Phys*. **1996**, *105*, 1052-1059.

Published as Adv. Synth. Catal. 2016, 358, 3231-3243. doi.org/10.1002/adsc.201600621

(22) Zhao, Y.; Truhlar, D. G. *Theor. Chem. Acc*. **2008**, *120*, 215-241.

(23) Schaefer, A.; Huber, C.; Ahlrichs, R.; *J. Chem. Phys*. **1994**, *100*, 5829-5835.

(24) (a) Barone, V.; Cossi, M. *J. Phys. Chem. A* **1998**, *102*, 1995-2001. (b) Tomasi, J.; Persico, M. *Chem. Rev*. **1994**, *94*, 2027-2094.

(25) (a) Poater, A.; Pump, E.; Vummaleti, S. V. C.; Cavallo, L. *J. Chem. Theory Comput*. **2014**, *10*, 4442-4448. (b) Pump, E.; Slugovc, C.; Cavallo, L.; Poater, A. *Organometallics* **2015**, *34*, 3107-3111; (c) Manzini, S.; Poater, A.; Nelson, D. J.; Cavallo, L.; Nolan, S. P. *Chem. Sci*. **2014**, *5*, 180-188.

(26) Advanced Inorganic Chemistry, ed. F. A. Cotton, G. Wilkinson, C. A. Murillo, E. M. Bochmann, Wiley, **2009**.

(27) Metzinger, R.; Limber, C Z. *Anorg. Allg. Chem*. **2012**, *638* (14), 2225-2234.

(28) (a) D'Elia, V.; Ghani, A. A.; Monassier, A.; Sofack-Kreutzer, J.; Pelletier, J. D. A.; Drees, M.; Vummaleti, S. V. C.; Poater, A.; Cavallo, L.; Cokoja, M.; Basset, J.-M.; Kuehn, F. E. *Chem. Eur. J.* **2014**, *20*, 11870-11882. (b) D'Elia, V.; Dong, H.; Rossini, A. J.; Widdifield, C. M.; Vummaleti, S. V. C.; Minenkov, Y.; Poater, A.; Abou-Hamad, E.; Pelletier, J. D. A.; Cavallo, L.; Emsley, L.; Basset, J.-M. *J. Am. Chem. Soc.* **2015**, *137*, 7728-7739.

Published as Adv. Synth. Catal. 2016, 358, 3231-3243. doi.org/10.1002/adsc.201600621

TABLE OF CONTENTS